ENCIT 2018

ABCM Associação Brasileira de Engenharia e Ciências Mecânicas

17th Brazilian Congress of Thermal Sciences and Engineering
November 25th-28th, 2018, Águas de Lindóia, SP, Brazil

NUMERIC EVALUATION OF A HEAT PIPE-RADIATOR ASSEMBLY FOR SPACE POWER SYSTEMS

Luis Felipe Ribeiro Romano
Aeronautics Institute of Technology, São José dos Campos, Brazil
luisromano_91@hotmail.com

Guilherme Borges Ribeiro
Institute for Advanced Studies, São José dos Campos, Brazil
Aeronautics Institute of Technology, São José dos Campos, Brazil
gbribeiro@ieav.cta.br

Abstract. *The research and technological development towards compact energy conversion systems for space applications allows the emergence of new mission possibilities, especially those directed for deep space explorations. Considering the Closed Brayton Cycle of as the energy conversion system for nuclear power, an analysis was conducted regarding the conversion cycle's Cold Side mass. The complete radiator assembly was separated in control volumes, considering variable geometry parameters for each of them, presenting a variable sized trapezoidal space radiator assembly as output. Each control volume is physically and thermally coupled with water heat pipe (HP). The heat flux was limited by the geometry of each panel section, being its heat pipe modeled to fit given geometry and verified against its operational limits. The model considered a geometric and thermal coupling with temperature drops along the heat pipe axial direction, the radiator panel surface – modeled as a radiative fin – and the heat exchanger duct, providing reasonable global parameters to aid the decision making of the radiator designer. The model showed feasible results within a range of 507K and 525K for the duct inlet temperature, with the first law cycle efficiency ranging between 20% and 25%. Considering the fixed wick and initial heat pipe geometry input provided, a heat pipe spacing of 0.05 ~ 0.15m and a radiation shield shadow's angle of 0 ~ 5° provided the lowest feasible heat pipe-radiator mass. Cold Side total masses of 600 to 800kg were observed, along with HP quantities ranging from 175 to 375 and a total radiator length of roughly 25m.*

Keywords: *radiator, heat pipe, space, Brayton cycle.*

1. INTRODUCTION

Energy conversion systems play an important role on generating usable electric energy in space, especially because most energy sources usually provide thermal, mechanical or chemical energy, and the proper use of the produced electricity is fundamental for the mission success. Due to this reason, high-power density and a full power availability – regardless of the ambient condition – are crucial aspects that make nuclear energy the chosen option for the long-range space exploration (Ashe et al., 1990). In addition, it is well known that weight is a factor that determines the feasibility of any project when directed to space applications, given the need to propel it from the ground using rocket launchers, therefore being a relevant property to be analyzed.

For any conversion system, an amount of unused heat must be extracted by the low temperature heat sink. In space, the heat rejection is typically performed by a set of radiators (RAD) attached to the cold side of the energy conversion system by Heat Pipes (HP), which are responsible for extracting heat from the conversion system working fluid and distribute it along the panels, where rejection to the external ambient occurs. As pointed out by other studies (Mason et al., 2002; Tarlecki et al., 2007), the heat pipe-radiator (HP-RAD) assembly commonly has the highest mass contribution on space power systems. Hence, it is a critical component which must be designed taking into account its mass and heat extraction capacity.

The Closed Brayton Cycle (CBC) is considered as a promising energy conversion system, since it promotes higher power output to radiator area ratio, when compared to other dynamic cycles (Tarlecki et al., 2007 and El-Genk, 2008). Considering these aspects, several studies have focused on the performance prediction of a CBC for space power systems (Bageenstoss and Ashe, 1992; Harty et al. 1993; Shaltens and Mason, 1996; Hyder et al., 2000; Mason, 2003). Ribeiro *et al*. (2015) described a CBC numeric model and, as did Juhasz (2007), pointed the space radiator as the most critical component to be dimensioned for the conversion's system feasibility.

To put it in perspective, a conceptual craft presenting two full radiator sets can be seen in Fig. 1, which was also used as ground reference for this work's model development. As commented previously, typical space radiators operate assisted by a set of Heat Pipes (HP) which are responsible for extracting heat from the CBC's working fluid and conducting to the panels (Wang *et al*, 2017; Zhang *et al*, 2016a and 2016b; Vlassov *et al*., 2006). Most of studies

considers the amount of heat needed to be extracted and the temperature range on which the HP is supposed to operate as fixed inputs, having the geometry, material, working fluid and thermal coupling as parameters to be studied and optimized. This approach allows to compare numeric results with experimental data provided that the component is being dimensioned alongside the model elaboration and optimization.

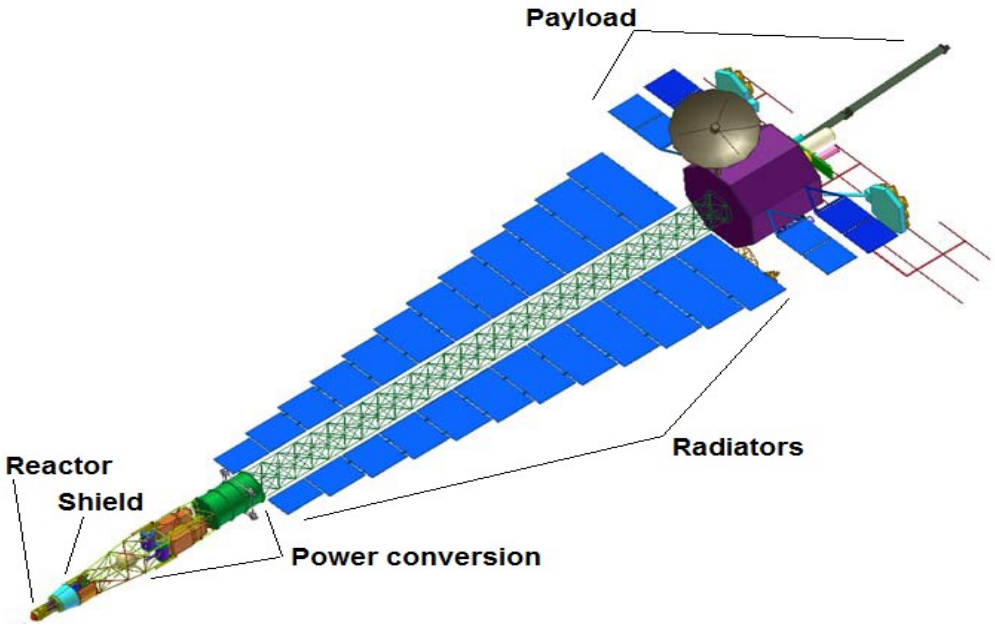

Fig. 1: Conceptual nuclear powered spacecraft design with two symmetrical radiator sets (Juhasz, 2007).

In their study, Ribeiro et al. (2015) performed an endoreversible modeling and optimization of a CBC as energy conversion system for nuclear space power systems. Both the HP and Cold Heat Exchanger (CHE) were represented by their individual overall thermal conductances, whereas a simple planar radiative heat transfer characterized the radiator. Additionally, the temperature drop along the CHE was neglected, determining a single temperature for its operation. Thus, a fixed temperature was applied in the radiator.

Juhasz (2005; 2007) described a mathematical model which considers variable-size radiator panels. The proposed analysis was valid for a pumped loop and for heat pipe heat exchangers. In his model, the temperature drop between the heat pipe evaporator and condenser was neglected, as well as the radiative panel efficiency. Comparison between rectangular and different trapezoidal shapes was performed.

Tomboulian (2014) proposed a model and then evaluated experimentally a lightweight radiator for nuclear electric propulsion vehicles. In order to decrease to total heat radiator mass, several low-density materials were tested. According to results, the radiator panel made of carbon fiber provided a substantial decrease of radiator area and mass, when compared to copper, molybdenum and carbon-carbon composite.

The works of Tomboulian (2014) and Juhasz (2007) considered simplifications such as iso-geometric radiator panels and isothermal radiative rejection with no temperature drop along the HP length. Those have provided useful data to their needs given the experimental aid to validate and correct the models. This work, on the other hand, has a theoretical approach and it is intended to serve as a design-based tool to size lightweight heat pipe-radiators which meet the energy conversion system requirements. Therefore, a model coupling the radiator, the cold side HP and heat transfer relations at the Cold Heat Exchanger (CHE) section by considering geometric and thermal parameters is proposed.

This work's model presents a temperature drop between each HP's evaporator and condenser, variable-sized radiator panels, HP condenser lengths and external diameters – all for a specific HP wick geometry. Furthermore, it also considers a temperature drop between each HP evaporator via an energy balance along the CHE, promoting a non-isothermal system with several temperature nodes.

Considering the operational temperature range (Romano and Ribeiro, 2017), titanium and water were chosen as material and working fluid of the heat pipes, respectively (Yang et al., 2012; Anderson et al., 2006). Thus, both the HP container and wick structure are made of titanium. Rectangular grooves were considered as the HP capillary wick, whereas for the radiator panel aluminum sheets were applied. The use of aluminum sheets may no longer be widespread for this kind of operation but its model description allows the evaluation of different materials with interesting properties in future studies (Tomboulian, 2014).

Initially, the model intend to generate data to evaluate which geometrical arrangement will provide the lowest total mass within a feasible length for the cold side of the CBC, therefore being of great interest to start a space radiator design and guiding the development of an operational rejection system within the predicted optimal range. The model

also enables to simulate chosen specifications and predict temperature drops and thermal behavior in each section of the CHE, as well as to evaluate overall system dimensions if needed in future applications. With a model that predicts the assembly thermal performance, a minimization algorithm provided by the solver was applied and reference values for some noteworthy parameters of the assembly were obtained, providing data to guide future experiments and designs during the engineering conception phase. In addition, it is important to bear in mind that any aspect regarding major manufacturing processes and structural analysis of such equipment are out of scope of this study, although being of extreme relevance and required to be evaluated before the final design of the components.

2. MATHEMATICAL MODEL

This work was developed to provide data for dimensioning the cold side of a CBC, such as radiator area, number of HP (N_{hp}) and their individual dimensions as well as the rejection system total mass (m_{sink}) and expected length (L_{sink}). The proposed model was conceived in a way it could be later coupled to another numeric description representing the complete CBC operation for future studies. The goal is to simulate the system operation and allow parametric variations in order to provide data to use as reference for design and guide future experiments. For conciseness and clarity, not all procedures included in the calculations will be discussed in this work.

The model used to represent the RAD panel operation associates the radiative heat transfer and an adapted fin efficiency correlation in order to determine the radiated heat by a geometrically defined panel. Initially, the radiator is separated in symmetrical sets by dividing the total value of heat that has to be rejected, determining how much is to be extracted by each set. The symmetry line intersects the CHE duct as shown in Fig. 2. Next, using a control volume (CV) description, each set is then subdivided in smaller sections around a single HP where its radiator panel dimensions are provided as input. Each panel is responsible to reject a certain amount of heat, directly proportional to its surface area, temperature of rejection and efficiency of operation while each HP has its own temperature gradient and involucre geometry, being determined to fit the its panel's thermal needs. The heat transfer rate extracted by each radiator element is calculated as follows:

$$Q_{rad}[n] = A_{rad} \cdot \eta_{rad} \cdot \sigma_{rad} \cdot \varepsilon_{rad} \cdot F_{rad} (T_{hp,cond}[n]^4 - T_{sp}{}^4) \tag{1}$$

where the A_{rad} is the radiator area, η_{rad} denotes the radiative fin efficiency, σ_{rad} is the Stefan-Boltzmann constant, ε_{rad} is the surface emissivity, whereas F_{rad} represents the form factor. Each section of radiator panel is represented using the heat transfer theory of finned surfaces, considering an adiabatic surface at the tip and a fixed temperature at the base $T_{hp,cond}$, placed at the heat pipe condenser. Temperature T_{sp} denotes the heat sink temperature, which represents the space. Applying an analogy between Eq. (1) and the Newton´s law of cooling, the radiation heat transfer coefficient is computed as

$$h_{rad} = \sigma_{rad} \cdot \varepsilon_{rad} \cdot F_{rad} \left(T_{hp,cond}[n]^2 + T_{sp}{}^2\right) \cdot \left(T_{hp,cond}[n] + T_{sp}\right) \tag{2}$$

For this analysis, the radiator panels, were represented as thin sheets of aluminum.

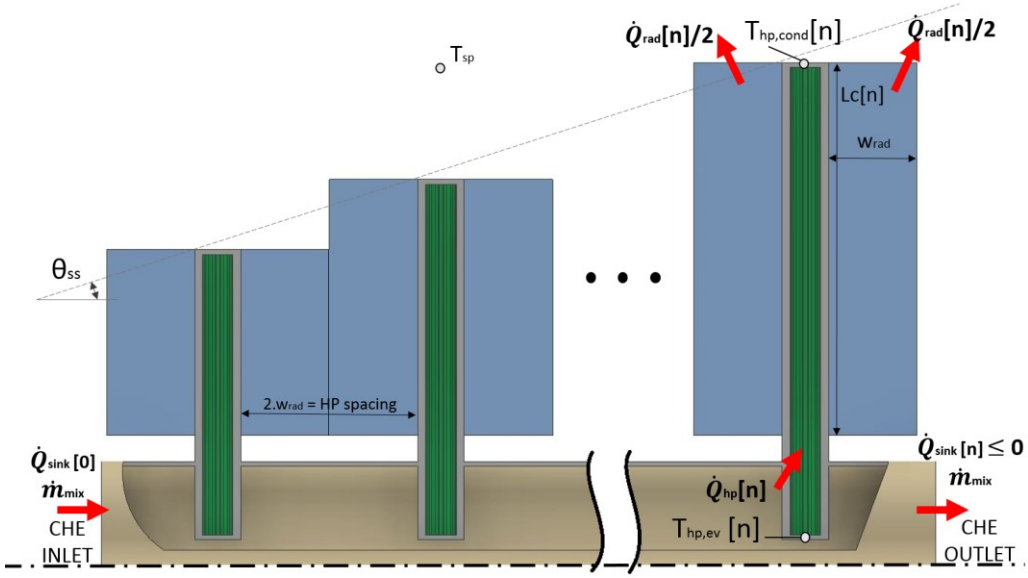

Fig. 2: Representation of the coupling model in a heat pipe-radiator assembly.

The description for the heat transfer occurring between the HP evaporator and condenser, as well as between any of its internal sections, is based on the thermal conductance method. The proposed model considers an association of thermal resistances related to each heat pipe component, one for each HP section, which also allows the computation of the temperature field along the HP, for a given heat transfer rate the pipe is subjected to. Axial symmetry was assumed, and a typical representation of the HP thermal conductances with their respective thermal conductances is shown in Fig. 3.

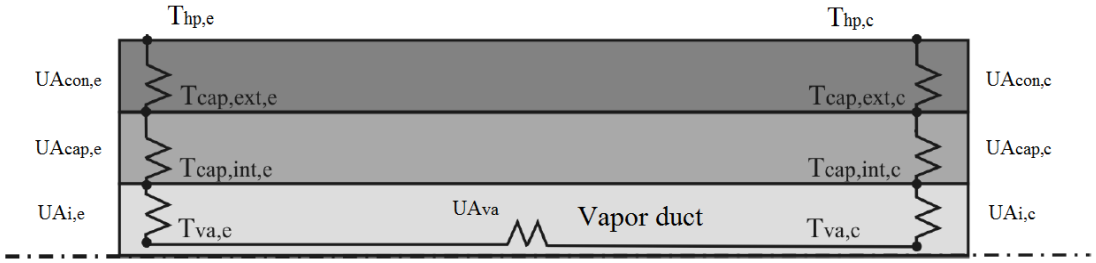

Fig. 3: Axisymmetric heat pipe thermal resistances.

The container and wick resistances in the adiabatic region were assumed negligible in this model. Hence, the heat pipe is modeled as a one-dimensional heat transfer case. The thermal conductances related to radial conduction of the container at the evaporating and condensing regions are defined as

$$UA_{con,e} = \left[\frac{1}{2\pi k_{con,e} L_e} ln\left(\frac{D_{con}/2}{D_{cap}/2}\right)\right]^{-1} \tag{3}$$

$$UA_{con,c} = \left[\frac{1}{2\pi k_{con,c} L_c} ln\left(\frac{D_{con}/2}{D_{cap}/2}\right)\right]^{-1} \tag{4}$$

Where k_{con} denotes the container thermal conductance. Variables D_{con} and D_{cap} represent the container and capillary wick external diameter, respectively, as shown in Fig. 4. The terms L_e and L_c are the evaporator and condenser length, respectively.

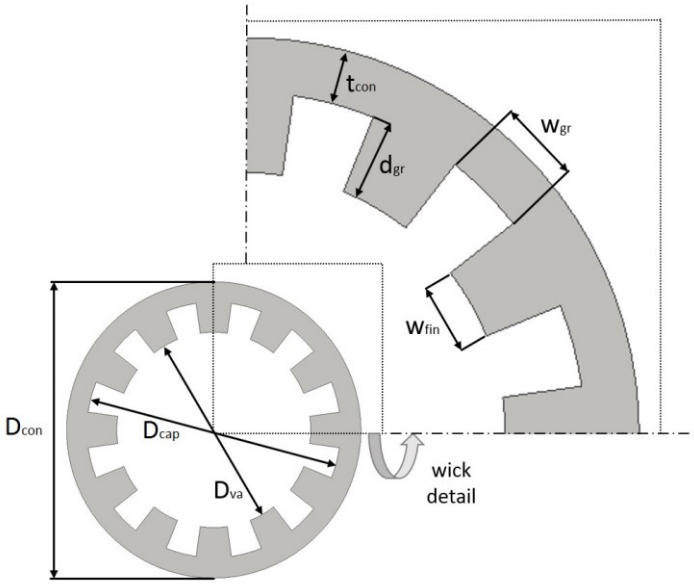

Fig. 4: Axisymmetric heat pipe thermal resistances.

The container thickness (t_{con}) is based upon its external diameter and calculated inwards using the Barlow's formula. It correlates the tensile stress of titanium σ_{ti} and the HP internal pressure, which is the saturation pressure P_{sat} at the HP maximum allowed temperature T_{max}, being it defined for this work as 10% above the HP evaporator temperature. Thus,

$$t_{con} = \frac{D_{con} - D_{cap}}{2} = \frac{P_{sat}[T_{max}]\, D_{con}}{2\,\sigma_{ti}} \tag{5}$$

Moreover, a lower thickness limitant of 0,25mm was introduced on the code to avoid extremely thin tubes obtained at lower saturation pressures. Above this threshold, the value was considered as calculated by the presented Eq. (5).

Similarly to Eqs. (3) and (4), the wick structure is also characterized by a axial conduction heat transfer. Thus, the thermal conductance present in the evaporator and condenser is represented as follows

$$UA_{cap,e} = \left[\frac{1}{2\pi k_{cap,e} L_e} ln\left(\frac{D_{cap}/2}{D_{va}/2}\right)\right]^{-1} \tag{6}$$

$$UA_{cap,c} = \left[\frac{1}{2\pi k_{cap,c} L_c} ln\left(\frac{D_{cap}/2}{D_{va}/2}\right)\right]^{-1} \tag{7}$$

Where $k_{cap,e}$ and $k_{cap,c}$ are the effective capillary wick thermal conductivity at the evaporating and condensing zones, respectively. The term D_{va} denotes the vapor duct diameter. The effective thermal conductivity is calculated as proposed by Ochterbeck (2003), as follows:

$$k_{cap} = \frac{(w_{fin}\, k_l\, k_{ti}\, d_{gr}) + w_{gr}\, k_l(0.185\, w_{fin}\, k_{ti} + d_{gr}\, k_l)}{(w_{gr} + w_{fin})(0.185\, w_{fin}\, k_{ti} + d_{gr}\, k_l)} \tag{8}$$

where w_{fin} denotes the fin width, whereas w_{gr} and d_{gr} denotes the groove width and depth, respectively. These variables characterize the groove profile, as shown in Fig. 4. The thermal conductivity of water and titanium are represented as k_l and k_{ti}, respectively. Faghri (1995) defines the thermal conductance related to the liquid-vapor interface at the evaporator and condenser based on the following equations:

$$UA_{i,e} = \left[\frac{R\, T_{va,e}^{\,2}\, \sqrt{2\,\pi\, R\, T_{va,e}}}{MW\; 2\,\pi\, L_e\, h_{lv,e}^{\,2}}\right]^{-1} \tag{9}$$

$$UA_{i,c} = \left[\frac{R\, T_{va,c}^{\,2}\, \sqrt{2\,\pi\, R\, T_{va,c}}}{MW\; 2\,\pi\, L_c\, h_{lv,c}^{\,2}}\right]^{-1} \tag{10}$$

where R is the ideal gas constant, MW is the water molecular weight and h_{lv} is the enthalpy of vaporization at the vapor duct temperature T_{va}, for each HP section. Moreover, the thermal conductance related to the vapor duct is detailed as

$$UA_{va} = \left[\frac{(P_{va,e} - P_{va,c})\left(\frac{T_{va,c} + T_{va,e}}{2}\right)}{h_{lv,va}\, \rho_{v,va}\, \dot{Q}_{hp}}\right]^{-1} \tag{11}$$

In Eq. 11, variable $P_{va,e}$ denotes the vapor saturation pressure for the temperature $T_{va,e}$, at the evaporator zone in the vapor duct, whereas $P_{va,c}$ is the vapor saturation pressure, for the condenser temperature $T_{va,c}$. The HP heat transport rate is $\dot{Q}_{hp}$ and the enthalpy of vaporization $h_{lv,a}$ and density $\rho_{v,va}$ were computed based on the average vapor temperature at the evaporator and condenser ($T_{va,e}$ and $T_{va,c}$).

Material and fluid properties were obtained using the library provided by the REFPROP software (McLinden et al., 1998), as function of the average temperature of the heat pipe section (i.e., evaporator and condenser). The temperature

drop ΔT_{hp} along a given HP [n] was computed based on the overall thermal conductance and considering the HP heat transfer rate $\dot{Q}_{hp}$ as follows:

$$\Delta T_{hp}[n] = \frac{\dot{Q}_{hp}[n]}{UA_{tot}[n]} \tag{12}$$

$$\frac{1}{UA_{tot}} = \frac{1}{UA_{con,e}} + \frac{1}{UA_{cap,e}} + \frac{1}{UA_{i,e}} + \frac{1}{UA_{va}} + \frac{1}{UA_{i,c}} + \frac{1}{UA_{cap,e}} + \frac{1}{UA_{con,c}} \tag{13}$$

Each HP operation is verified against its operational limits, as described in several studies (Reay *et al*., 2014). The evaluation takes into account the failure limits (capillary, boiling and entrainment) and the non-failure limits (sonic and viscous), whereas the condenser limit is utilized for the coupling process. A safety factor is considered, requiring that the dimensioned HP is able to conduct at least twice of the heat rejected by the RAD panel coupled to it.

If the limit verification fails, the code increments the HP container diameter by 10% of the minimum threshold (i.e., 0.015 m), and a new iterative procedure starts for the same CV. This increment is repeated until a valid thermal coupling is obtained or when the provided maximum diameter is extrapolated (i.e., 0.200 m), being the HP-RAD element of that CV flagged as not operational, requiring a reevaluation on the initial parameters.

The described model is incremental and will add new HP-RAD elements along the CHE duct until the thermal needs for this CBC component is met. For each CV, the HP with the smaller container diameter capable of meeting the panel's thermal needs is selected, providing always the lighter HP possible for that assembly element.

3. RESULTS

The solver used to compile the models presented on this work provides a variable minimization tool on its environment (Klein and Alvarado, 1993), which concedes five already implemented algorithms for minima determination. For a non-linear system solution, the Nelder-Mead simplex method (Lagarias et al., 1998) presented good response and convergence behavior for the implemented models. Thereat, a m_{sink} minimization procedure was conducted and specific values for N_{hp} and L_{sink} were prompted for an optimal $T_{che,in}$ (i.e. CHE inlet temperature). Nine cases were considered by varying η_{cbc} = (0.15, 0.20, 0.25) and θ_{ss} = (0°, 5°, 10°), while allowing both HP spacing and $T_{che,in}$ to float between 0.1 ~ 0.5m and 500 ~ 550K, respectively. Guide curves were drawn by the solver to link the points with the same θ_{ss} however, since the free variables were left to float during minimization, it is noteworthy to point that their overall behavior serves more as reference than actual intermediate results within the efficiency range.

The behavior of N_{hp} as function of the efficiency for all nine evaluated cases is presented in Fig. 5. For a θ_{ss} of 0°, the number of heat pipes varied around 1000 unities for all three η_{cbc} (0.15, 0.20 and 0.25), reaching over 1000 unities for efficiencies lower than 22%, as induced by the approximate curve. For θ_{ss} of 5° and 10° N_{hp} dropped considerably, falling within the range of 125 to 375 HP. Of the three cases run for θ_{ss} = 5°, the minimum value observed was at η_{cbc} = 0.20, increasing even for higher efficiencies. At 10°, N_{hp} was reduced with the increase of the CBC efficiency.

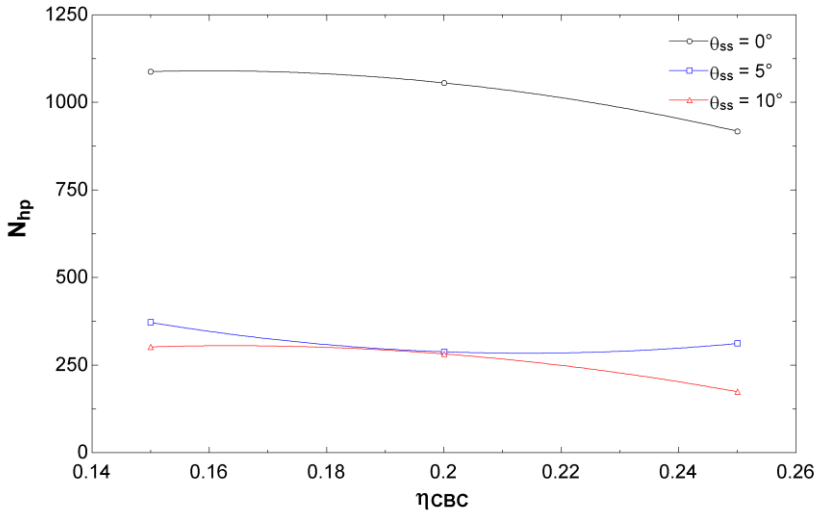

Fig. 5: Encountered N_{hp} for all nine cases as function of η_{cbc}.

Fig. 6 shows that shorter assemblies are achievable by lowering θ_{ss}. The values presented almost no variation of length for θ_{ss} of 5° and 10°, which can be justified by the code operation of altering the HP diameter or even by the variation of HP spacing to reach the minima for each case (Fig. 7), which alters the total amount of rejected heat by each section. It can be pointed that lower values of θ_{ss} tend to result on longer and impractical HP-RAD assemblies.

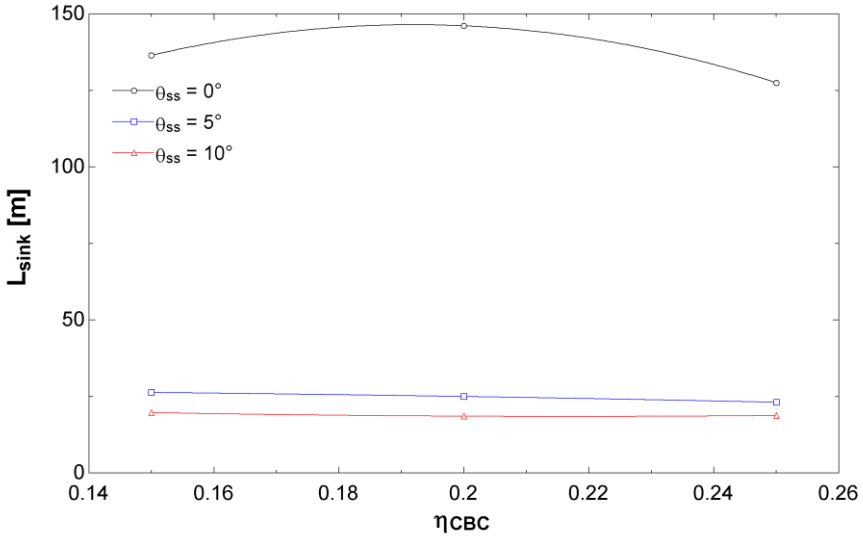

Fig. 6: Encountered L_{sink} for all studied cases as function of η_{cbc}.

As pointed before, Fig. 7 elaborates on the behavior of the optimal HP spacing variation while considering the nine cases studied in this section. For a θ_{ss} of 0°, the HP spacing of 0.2 to 0.25m were the ones who presented points of minimum mass for all three evaluated η_{cbc}. With a higher shadow angle introduced, the minima solutions tended to be found around 0.1 and 0.15m, however θ_{ss} = 10° presented a tendency to increase the optimal spacing in order to maintain a low mass arrangement in higher efficiencies.

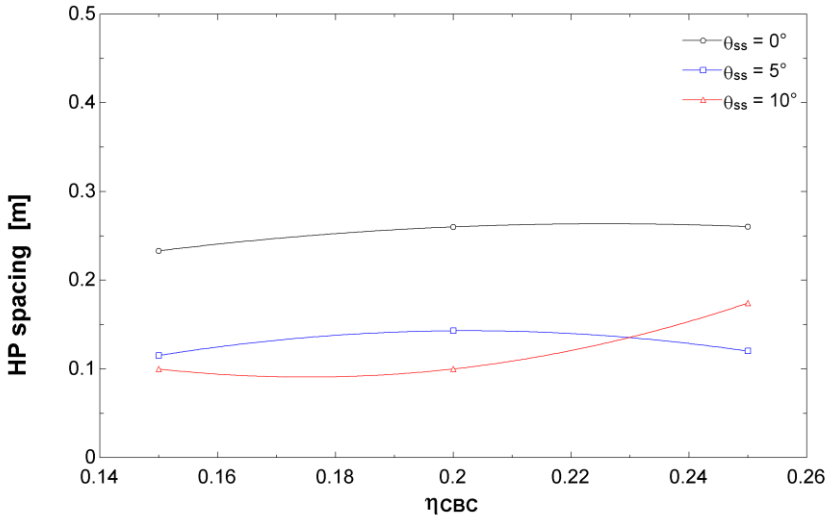

Fig. 7: HP spacing behavior for all cases as function of η_{cbc}.

The optimal CHE inlet temperatures for a lightweight HP-RAD assembly are depicted in Fig. 8. It points that inlet temperatures of 520 to 535K are expected considering a θ_{ss} of 0°, while a lower range of 505 to 515K is indicated for angles of 5° and 10°. An angle of 5° presented the lower values for inlet temperature or efficiencies lower than 20%, whereas 10° presented the lowest point of all cases for higher η_{cbc}.

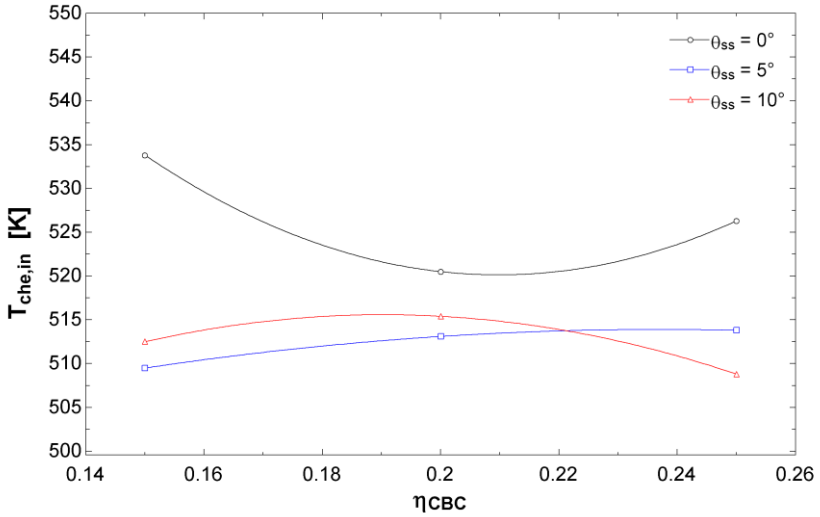

Fig. 8: Expected CHE inlet temperature within the cases range as function of η_{cbc}.

Finally, the resulting mass values for all nine optimization cases are illustrated in Fig. 9. As observed, higher efficiencies will provide lower values for the total mass while higher shadow angles will provide shorter but somewhat heavier assemblies, being expected weights of 700 to 800kg for assemblies with a θ_{ss} of 10° and as low as 400 to 450kg for those which θ_{ss} = 0°.

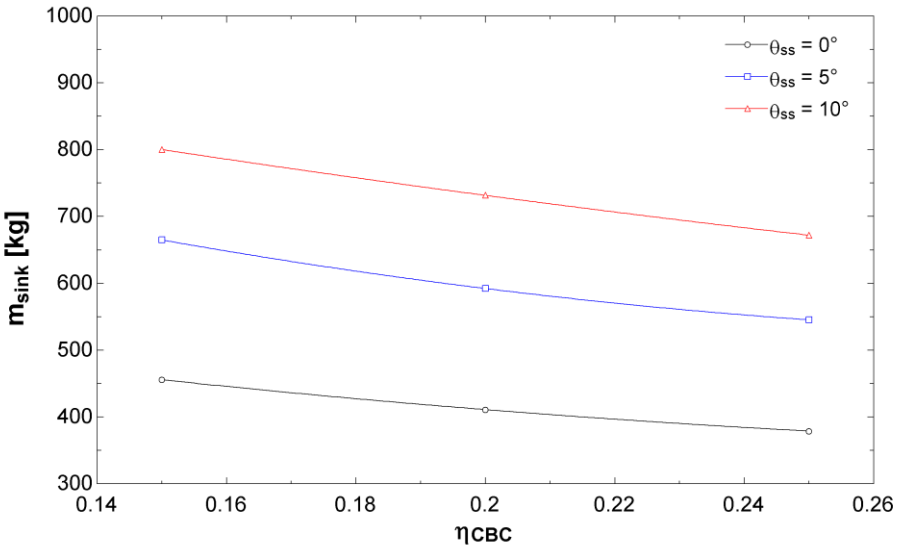

Fig. 8: Expected cold side mass behavior considering the studied cases.

4. CONCLUSIONS

The algorithm developed to represent the CBC's Cold Side operation and the geometric and thermal coupling of the titanium-water HP with the radiator panels and the CHE He-Xe gaseous mixture flow is functional and presented reasonable thermophysical behavior, as far as the analysis presented. Since the thermal operation is coupled to the HP-RAD assembly geometry, the performance prediction will drastically change if any input parameter is altered. For that reason, the proposed parametric evaluation provides a good understanding of the system's model behavior and can be used alongside the engineering design.

Results have shown that the number of heat pipes is reduced when the heat pipe spacing in increased. It can be induced that bigger radiator panels will reject more heat given a bigger surface area available for radiative heat transfer, reducing the total number of assembly elements that need to be iterated to fulfil the heat extraction requirement. With

the reduction of the HP quantity the overall system's mass should diminish as well, however the mass reduction is attenuated by the need of bigger HP needed to compensate for the higher heat fluxes.

Regarding the minimization tool, the Nelder-Mead method provided optimal results for lightweight HP-RAD assemblies with masses around 600 to 700kg for assemblies with a θ_{ss} of 5°. A tradeoff of mass and length can be observed through the minimization procedure, demonstrating that a lighter craft tends to be longer than a heavier one. Practical lengths of around 25m were observed as well as N_{hp} of 175 to 375 for a symmetrical HP-RAD assembly and a CHE inlet temperature of 507 to 525K is to be expected on such designs.

The mass/length tradeoff is a relevant parameter to be analyzed during design, and an optimal point is to be determined for each HP material and fluid selected, as well as for each assembly geometry and radiator panel material. Given the data presented in this study, it can be concluded that feasible crafts are achievable within a θ_{ss} of 0 ~ 5°, a $T_{che,in}$ of 507 ~ 525K, a N_{hp} of 175 ~ 375 unities, a L_{sink} of roughly 25m, a HP spacing ranging between 0.05 ~ 0.15m and a m_{sink} of 600 ~ 800kg, while aiming for CBC efficiencies higher than 20%.

Additionally, all curves and data generated by the operation of this numeric model can provide aid for the radiator development as intended, allowing the designer to understand the consequences of each geometric modification on the thermal operation. The model itself can be fed with the geometric layout and contour conditions as input and the approximate thermal operation of each element is provided as reference.

5. REFERENCES

Anderson W., Dussinger P., Bonner R., Sarraf D., "High Temperature Titanium/Water and Monel/Water Heat Pipes", 4th Int. Energy Convers. Eng. Conf. Exhib., 2006. doi:10.2514/6.2006-4113.

Ashe T. L., Baggenstoss W. G., Bons R., "Nuclear Reactor Closed Brayton Cycle Power Conversion System Optimization Trends for Extra-Terrestrial Applications", Intersociety Energy Conversion Engineering Conference, Reno, 1990.

Baggenstoss W. G., Ashe T. L., "Mission Design Drivers for Closed Brayton Cycle Space Power Conversion Configuration", ASME Journal of Engineering for Gas Turbines and Power, pp. 721-726, 1992.

El-Genk M. S., "Space Nuclear Reactor Power System Concepts with Static and Dynamic Energy Conversion", Energy Conversion and Management, v. 49, pp. 402-411, 2008.

Harty R. B., Otting W. D., Kudija C. T., "Applications of Brayton Cycle Technology to Space Power", Intersociety Energy Conversion Engineering Conference, Washington, DC, 1993.

Hyder A. K., Wiley R. L., Halpert G., Flood D. J., Sabripour S., "Spacecraft Power Technologies", Imperial College Press, London, pp. 332-340, 2000.

Juhasz A., "Heat Transfer Analysis of a Closed Brayton Cycle Space Radiator", 5th Int. Energy Convers. Eng. Conf. Exhib., 25–27, 2007. doi:doi:10.2514/6.2007-4841.

Juhasz A.J, "Analysis and numerical optimization of gas turbine space power systems with nuclear fission reactor heat sources", Phd Thesis, Cleveland State University, 2005.

Klein S. A., Alvarado J. L., "Engineering Equation Solver", F-Chart, 1993.

Lagarias J. C., Reeds J. A., Wright M. H., Wright P. E., "Convergence Properties of the Nelder–Mead Simplex Method in Low Dimensions *," vol. 9, no. 1, pp. 112–147, 1998.

Mason L. S.,"A Power Conversion Concept for the Jupiter Icy Moons Orbiter", International Energy Conversion Engineering Conference, Reston, 2003.

Mason L. S.,"A Power Conversion Concept for the Jupiter Icy Moons Orbiter", International Energy Conversion Engineering Conference, Reston, 2003.

Ribeiro G. B., Braz Filho F. A., Guimarães, L. N. F., "Thermodynamic analysis and optimization of a Closed Regenerative Brayton Cycle for nuclear space power systems", Appl. Therm. Eng., v. 90, pp. 250–257, 2015. doi:10.1016/j.applthermaleng.2015.06.093.

Romano L. F. R., Ribeiro G. B., "Optimal Temperature of Operation of the Cold Side of a Closed Brayton Cycle for Space Nuclear Propulsion", International Nuclear Atlantic Conference, Belo Horizonte, 2017.

Shaltens R. K., Mason L. S., "Early Results from Solar Dynamic Space Power System Testing", AIAA Journal of Propulsion and Power, pp. 852-858, 1996.

Tarlecki J., Lior N., Zhang N., "Analysis of Thermal Cycles and Working Fluids for Power Generation in Space", Energy Conversion and Management, v. 48, pp. 2864-2878, 2007.

Tomboulian B. N., “Lightweight, High-Temperature Radiator for In-Space Nuclear-Electric Power and Propulsion“, Phd Thesis, University of Massachusetts Amherst, 2014.

Vlassov V. V., Sousa F. L., Takahashi W. K., “Comprehensive optimization of a heat pipe radiator assembly filled with ammonia or acetone“, Int. J. Heat Mass Transf. , v. 49, pp. 4584–4595, 2006. doi:10.1016/j.ijheatmasstransfer.2006.02.059.

Wang C., Chen J., Qiu S., Tian W., Zhang D., Su G. H., “Performance analysis of heat pipe radiator unit for space nuclear power reactor“, Ann. Nucl. Energy., v. 103, pp. 74–84, 2017. doi:10.1016/j.anucene.2017.01.015.

Yang X, Yan Y. Y., Mullen D., “Recent developments of lightweight, high performance heat pipes“, Appl. Therm. Eng., v. 33–34, pp. 1–14, 2012. doi:10.1016/j.applthermaleng.2011.09.006.

Zhang W., Wang C., Chen R., Tian W., Qiu S., Su G. H., “Preliminary design and thermal analysis of a liquid metal heat pipe radiator for TOPAZ-II power system“, Ann. Nucl. Energy, v. 97, pp. 208–220, 2016a. doi:10.1016/j.anucene.2016.07.007.

Zhang W., Zhang D., Tian W., Qiu S., Su G. H., “Thermal-hydraulic analysis of the improved TOPAZ-II power system using a heat pipe radiator“, Nucl. Eng. Des., v. 307, pp. 218–233, 2016b. doi:10.1016/j.nucengdes.2016.07.020.